

Electronic Supporting Information (ESI) for **Mechanochemical Synthesis of Cooperative Spin Crossover Materials**

J. H. Askew and H. J. Shepherd*

Contents:

- Full Experimental Details
 - Synthesis of Complexes **1-4**
 - Characterization
- Additional discussion of complex **1**
 - Magnetometry
 - Variable temperature Raman spectroscopy
 - Powder X-ray diffraction
 - FTIR
 - Thermal analysis
- Additional discussion of complex **2**
 - Effect of washing the sample for purification
 - Magnetometry
 - Variable temperature Raman spectroscopy
 - Powder X-ray diffraction
 - FTIR
 - Thermal analysis
- Variable temperature Raman spectroscopy of complex **3**
- Results and discussion of complex **4**
 - Magnetometry
 - Variable temperature Raman spectroscopy
 - Powder X-ray diffraction
 - FTIR

Full Experimental Details

Synthesis:

All reagents were purchased from Fisher Scientific, with the exception of $\text{Fe}(\text{BF}_4)\cdot 6\text{H}_2\text{O}$, which was purchased from Sigma Aldrich; all reagents were used as received. All mechanochemical experiments were conducted in air at ambient conditions.

For complexes **2** and **3**, the solution-state behaviour was assessed from literature reports and compared to the mechanochemically prepared samples as described in the main text. For complexes **1** and **4** we synthesized our own solution-state samples for comparison with those made via mechanochemistry due to conflicting reports or no magnetometry data being available in the literature.

CAUTION: Do not use mechanochemical techniques for the preparation of potentially explosive materials. Perchlorate salts and tetrazole ligands are occasionally used in SCO research. Both of these have the potential to explode when handled dry, particularly on contact or grinding, and should thus not be used in routine mechanochemical experiments. Care should also be taken when preparing cyanometallate complexes to avoid accidental release of cyanide.

Note on Elemental Analysis

As discussed in the main article, due to the nature of the mechanochemical procedure, the final product may well contain traces of unreacted starting materials and by-products from the reaction. The effect of washing the product to remove impurities is discussed in below detail for complex **2**. Calculated values for elemental analysis discussed below were based on likely compositions of the product at each stage, but should be interpreted with a degree of caution.

Complex **1**:

(**1**_{mech}): $\text{Fe}(\text{atrz})_3(\text{SO}_4)$, was prepared by grinding ammonium iron(II) sulfate hexahydrate (1.00 g, 2.55 mM) and 4-amino-4h-1,2,4-triazole (0.65 g, 7.73 mM) in an agate pestle and mortar in the absence of solvent. Immediately after grinding started, the sample became a wet purple paste. On continued grinding, the mixture dried to form a fine purple powder. CHN analysis for $[\text{Fe}(\text{atrz})_3](\text{SO}_4)\cdot 0.5(\text{NH}_4)_2(\text{SO}_4)\cdot 2\text{H}_2\text{O}$ found (calc). C 14.95 (14.24), H 3.97 (3.98), N 35.06 (35.97). Further drying was carried out at 200°C for 10hrs, to form the sample **1**_{mech}. CHN analysis for $[\text{Fe}(\text{atrz})_3](\text{SO}_4)\cdot 0.5(\text{NH}_4)_2(\text{SO}_4)$ found (calc). C 14.13 (15.33), H 3.32 (3.43), N 32.52 (38.72). A fraction of the sample prior to high temperature drying was washed using water and ethanol, filtered and dried under vacuum, CHN analysis for $[\text{Fe}(\text{atrz})_3](\text{SO}_4)\cdot 2\text{H}_2\text{O}$ found (calc): C 16.75 (16.37), H 3.11 (3.66), N 34.79 (38.19).

(**1**_{sol}): $[\text{Fe}(\text{atrz})_3](\text{SO}_4)$ was also prepared in aqueous solution; ammonium iron(II) sulfate hexahydrate (0.41 g, 1.05 mM) was dissolved in water (1.5 ml) then an excess of 4-amino-4h-1,2,4-triazole (0.51 g, 6.07 mM) in water (3 ml) was added dropwise. The mixture was stirred overnight; the precipitate was collected by filtration then dried under vacuum overnight yielding a purple powder. CHN analysis for $[\text{Fe}(\text{atrz})_3](\text{SO}_4)\cdot 2\text{H}_2\text{O}$ found (calc). C 16.66 (16.37), H 4.02 (3.66), N 41.73 (38.19).

While using $\text{Fe}(\text{SO}_4)\cdot 6\text{H}_2\text{O}$ as the source of Fe^{2+} may well reduce the presence of by-products in the mechanochemical reaction, it results in pronounced oxidation of the iron centres in the solution-based experiment. Such oxidation was not observed when using $[\text{NH}_4]_2[\text{Fe}(\text{SO}_4)_2]\cdot 6\text{H}_2\text{O}$, allowing direct comparison

between solution and mechanochemical techniques. It should however be noted that the product **1_{mech}** may contain ammonium sulphate impurities, as indicated by elemental analysis.

Complex 2:

[Fe(phen)₃](NCS)₂, **2_{pre}**, was prepared by grinding iron(II) tetrafluoroborate hexahydrate (0.50 g, 1.48 mM), 1,10-phenanthroline (0.70 g, 3.88 mM) and potassium thiocyanate (0.33 g, 3.40 mM) in an agate pestle and mortar in the absence of solvent. Within 1 minute the powder changed color from white to red. With continued grinding, a gradual color change was observed turning from red to an almost black powder. CHN analysis for [Fe(phen)₃](NCS)₂·0.15(Fe(BF₄)₂·6H₂O)·0.63KSCN·2KBF₄ found (calc). C 42.50 (41.85), H 2.43 (2.39), N 11.03 (11.50). The calculated formula is based on the assumption that everything in the reactants remained in the product.

Thermal conversion of [Fe(phen)₃](NCS)₂ to the spin crossover active complex Fe(phen)₂(NCS)₂, **2_{mech}**, was carried out by adapting a previously reported method.¹ The powder was heated to 80°C for 3 hours followed by high temperature drying at 200°C for 10 hours. The powder sample changed color from black to dark purple. CHN analysis for [Fe(phen)₂(NCS)₂]·0.15(Fe(BF₄)₂)·0.63KSCN·2KBF₄ found (calc). C 34.84 (36.35), H 1.82 (1.83), N 9.74 (10.55). A portion of the product was washed with water and ethanol, filtered and dried under vacuum, yielding a purple powder. CHN analysis for [Fe(phen)₂(NCS)₂]·KBF₄ found (calc). C 46.85 (47.44), H 2.36 (2.45), N 12.97 (12.77). A portion of the product was further washed with water and ethanol using sonication, filtered and dried under vacuum, yielding a purple powder. CHN analysis for [Fe(phen)₂(NCS)₂]·0.5KBF₄ found (calc). C 52.23 (52.45), H 2.59 (2.71), N 13.90 (14.12).

Complex 3:

{Fe(pz)[Au(CN)₂]₂} was prepared by grinding iron(II) tetrafluoroborate hexahydrate (0.17 g, 0.50 mM), pyrazine (0.04 g, 0.50 mM) and potassium dicyanoaurate(I) (0.30 g, 1.04 mM) in an agate pestle and mortar in the absence of solvent. Within 1 minute the powder changed formed a brownish red paste. After 5 minutes grinding the paste turned red. The paste was left to dry then ground into a powder, yielding a fine red powder, **3_{mech}**. CHN analysis for Fe(pz)[Au(CN)₂]₂·0.04KAu(CN)₂·2KBF₄·1H₂O found (calc). C 9.84 (10.94), H 0.36 (0.68), N 8.79 (6.44). The calculated formula is based on the assumption that everything in the reactants remained in the product.

Complex 4:

(**4_{mech}**): Fe(atrz)₃(BF₄)₂, was prepared by grinding iron(II) tetrafluoroborate hexahydrate (1.00 g, 2.96 mM) and 4-amino-4h-1,2,4-triazole (0.81 g, 9.63 mM). Immediately after grinding was started, the sample became a wet paste. After continued grinding, the mixture dried and became an off-white powder. CHN analysis for [Fe(atrz)₃](BF₄)₂·0.08(atrz)·1H₂O found (calc). C 15.04 (14.61), H 2.51 (2.85), N 34.76 (34.07). A portion of the product was dried at 225°C for 10hrs, to form **4_{mech}**. CHN analysis for [Fe(atrz)₃](BF₄)₂·0.08(atrz) found (calc). C 16.88 (15.15), H 2.20 (2.54), N 34.16 (35.33). A second portion of the product before drying was washed using water and ethanol, filtered and dried under vacuum, yielding a white powder CHN analysis for [Fe(atrz)₃](BF₄)₂·1H₂O found (calc). C 16.76 (14.42), H 2.31 (2.82), N 33.95 (33.64).

(**4_{sol}**): [Fe(atrz)₃](BF₄)₂ was also prepared from aqueous solution, iron(II) tetrafluoroborate hexahydrate (0.51 g, 1.5 mM) was added to 4-amino-4h-1,2,4-triazole (0.52 g, 6.2 mM) in water (5 ml). The mixture was stirred and the precipitate was collected by filtration then dried overnight yielding a white powder.

Additional Results and discussion

Complex 1:

The family of 1D triazole-based SCO coordination polymers are known to be sensitive to the presence of solvents, and especially water, in the lattice.² During the mechanochemical procedure water is liberated from the hydrated metal salt and forms a paste during grinding, as described in the experimental section as well as in the main text of the paper. Figure S1 shows the effect of residual water in the lattice from the synthesis on the magnetic properties, and Figure S2 shows the effect of washing the sample with water/ethanol on the same. While the effect of water on the transition is clearly significant a full characterisation of these effects is beyond the scope of the current study. As a consequence high temperature drying (below the melting point of the complex) was carried out to ensure traces of water were removed from the final product presented in the main text.

The effect of residual water is further investigated with Raman spectroscopy (shown in S3, S4 and S5), powder XRD (shown in Figure S6) and FTIR spectroscopy (Figure S7). Despite the significant differences in the magnetic data, the Raman and XRD data suggest similar structures in each case. Differences in the XRD pattern after high temperature drying may well indicate the removal of water from the lattice or relaxation of lattice strain caused by the significant structural rearrangement that occurs during SCO. After high-temperature drying, the solvent-synthesised product also showed significant differences in the diffraction pattern, as shown in Figure S6. Thus the process does not appear to be linked directly to the mechanochemical procedure, but is rather an intrinsic property of the material. It should be noted that during the first thermal cycle of the SCO, the hysteresis width is noticeably higher than on subsequent cycles. Whether these processes are related is the subject of further work.

A TGA plot showing the effect of heating at high temperatures is shown in Figure S8. The sample was heated from 25 to 450 °C at 5 °C/min with a 1 hour isotherm at 200°C whilst under a nitrogen atmosphere. The isotherm replicated the high temperature drying process. During this isotherm, 6% mass was lost, attributed to the loss of water. At the end of the isotherm, mass is still being lost. This suggested the removal of water was not complete after 1 hour. Thus the drying process for the bulk 1_{mech} sample was carried out for 10 hours so as to remove residual water from the system.

The use of washing the sample as a means to remove residual impurities is investigated further for complex 2 (vide infra), which is not known to be sensitive to the presence of water.

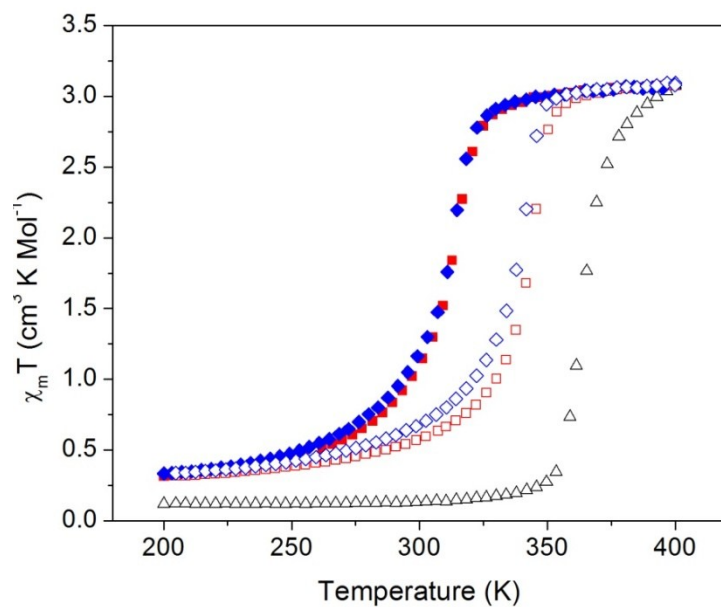


Figure S1: Squid data for $\mathbf{1}_{\text{mech}}$ prior to high temperature drying. Δ Cycle 1 Heat, \blacklozenge Cycle 2 Cool, \ast Cycle 2 Heat, \blacklozenge Cycle 3 Cool, \ast Cycle 3 Heat.

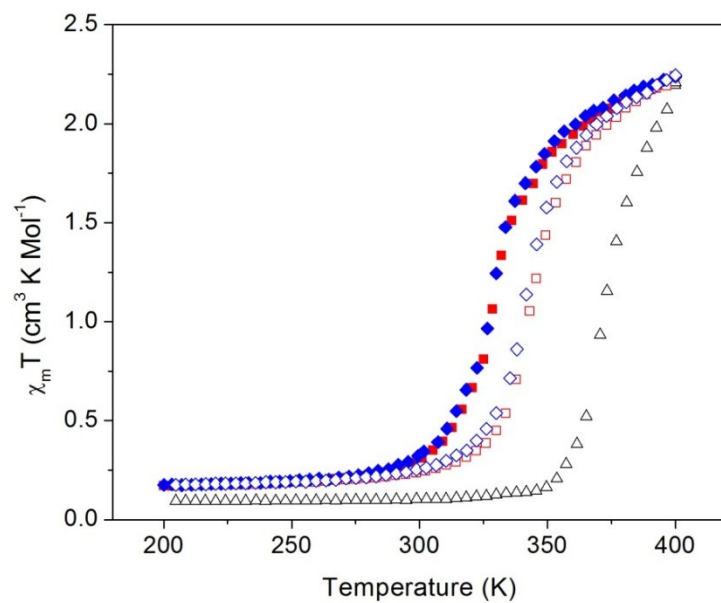


Figure S2: 3 Cycle Squid data for $\mathbf{1}_{\text{mech}}$ immediately after washing. Δ Cycle 1 Heat, \blacklozenge Cycle 2 Cool, \ast Cycle 2 Heat, \blacklozenge Cycle 3 Cool, \ast Cycle 3 Heat.

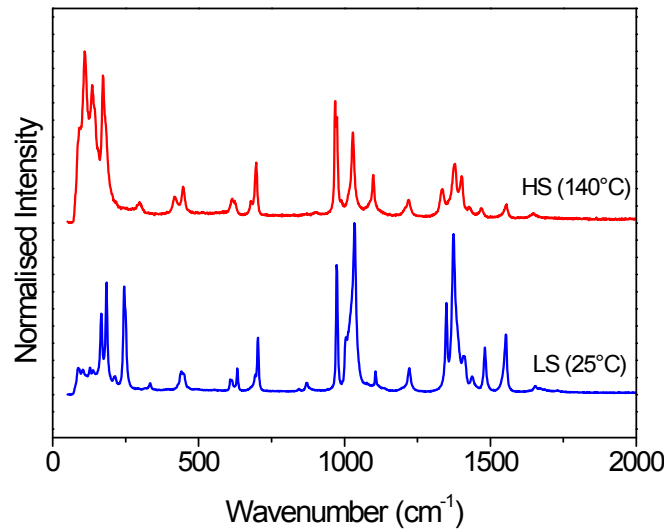


Figure S3: HS/LS Raman spectra for **1_{mech}** prior to high temperature drying.

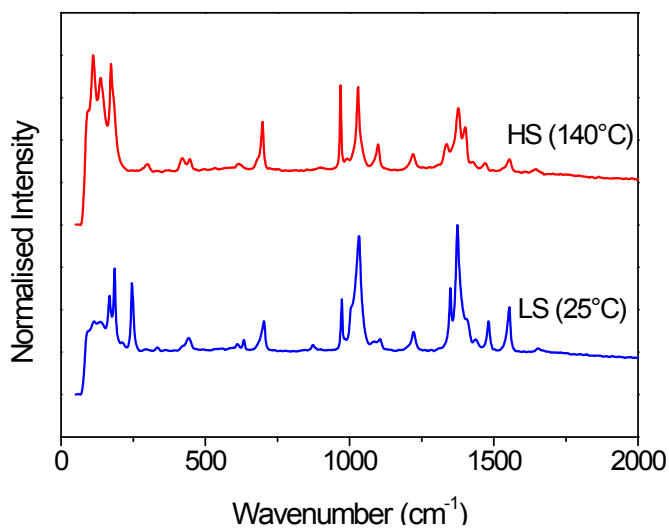


Figure S4: HS/LS Raman spectra for **1_{mech}** after high temperature drying.

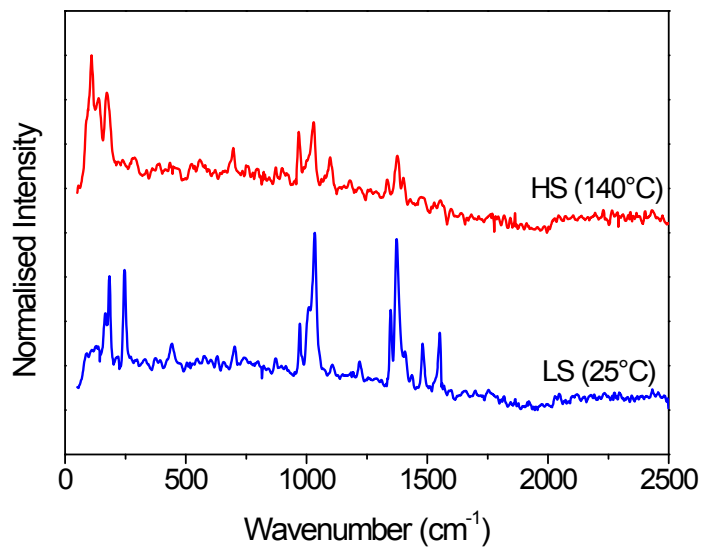


Figure S5: HS/LS Raman spectra for **1_{mech}** after washing in HS (top) and LS (bottom) states.

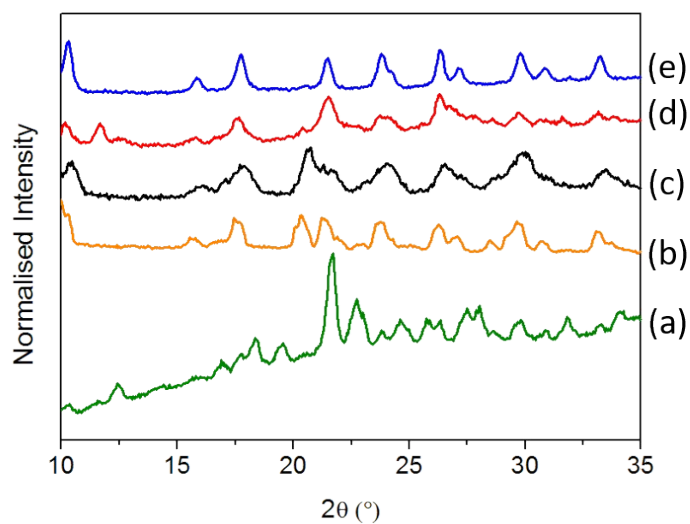


Figure S6: PXRD Patterns for **1**. (a) **1_{sol}** after high temperature drying, (b) **1_{sol}** before high temperature drying (c) **1_{mech}** before high temperature drying, (d) **1_{mech}** after high temperature drying, (e) **1_{mech}** after washing.

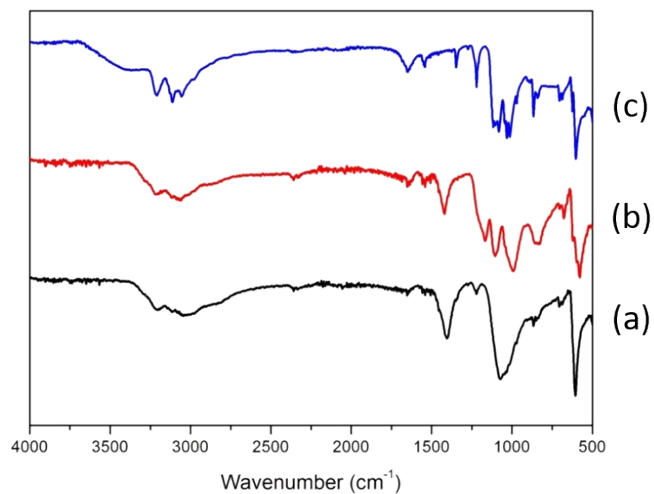


Figure S7: FTIR Spectra for **1**. (a) **1_{mech}** before high temperature drying, (b) **1_{mech}** after high temperature drying, (c) **1_{mech}** after washing.

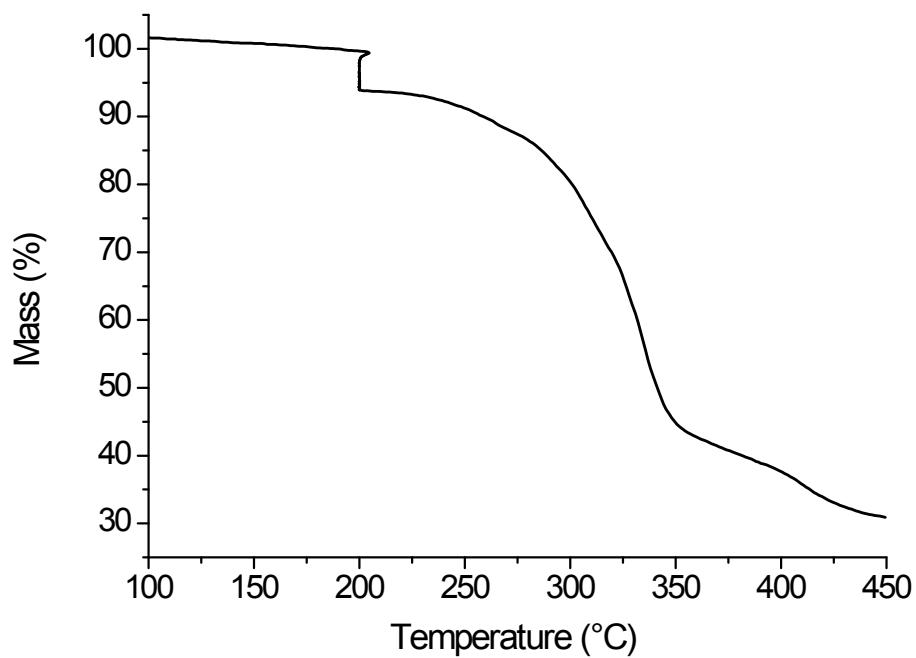


Figure S8: TGA plot for **1_{mech}** after grinding, without high temperature drying. Heated 25 to 450°C at 5°C/min with a 1 hour isotherm at 200°C.

Complex 2:

Fe(phen)₂(NCS)₂

The magnetic properties of the molecular compound Fe(phen)₂(NCS)₂ are relatively insensitive to the presence of solvents. As a consequence, the effect of washing the sample to remove residual impurities was able to be investigated without inducing potential solvent effects. As previously described, a fraction of mechanically prepared Fe(phen)₂(NCS)₂ was washed with water and ethanol then dried under vacuum. The resulting sample was analyzed using magnetometry (Figure S9) and PXRD (Figure S10). The magnetic properties of the sample were not significantly altered by the washing process, the transition temperature was only altered by 1 K ($T_{1/2}^{\text{LS}} = T_{1/2} = 175$ K), remaining within the range previously reported. The transition after washing was slightly more abrupt ('Smoothness' = 9 compared to 16 for the unwashed product), this is attributed to the removal of impurities and likely the loss of smaller particles during filtration. The difference in $\chi_m T$ between HS and LS states was also increased after washing; this was likely the result of impurity removal, which improved the accuracy of the M_w used in the calculation. Comparison of powder diffraction patterns for the sample before and after washing (Figure S10(c) and (d) respectively) show virtually no difference in crystallinity or structure of the material as a result of washing. The exception is the removal of peaks in the range 25 - 30° 2 θ on washing, attributed to the removal of impurities also observed in the PXRD pattern of the **2_{pre}** sample. Potential impurities may include by-products such as KBF₄.

Variable temperature Raman spectra for **2_{mech}** before and after washing are shown in Figures S11 and S12 respectively. No significant differences can be observed, revealing that the active compound is not affected by the washing process. As a consequence we conclude that washing to remove impurities is possible and does not change the nature of the active material unless it is inherently sensitive to the solvent as in the case of **1**. This highlights one of the major benefits of the mechanochemical process; avoiding solvents during preparation of the material allows the assessment of properties without the influence of host-guest interactions, which can be highly dependent on the exact synthetic protocol, and are often difficult to quantify and evaluate definitively.

TGA showing the conversion of **2_{pre}** to **2_{mech}** by thermolysis is shown in Figure S14. H₂O loss at 80°C isotherm was calculated by assuming all mass lost was H₂O and no H₂O remained in the sample. The remaining mass percentage, $\approx 92.6\%$, must then be [Fe(phen)₃](SCN)₂, $M_w = 911.55$ g/mol. M_w at 100% must then be = 1002.36 g/mol. The mass loss, $M_w = 90.81$ g/mol, was calculated to be the equivalent of approximately ≈ 5.05 moles of water per mole of [Fe(phen)₃](SCN)₂. The loss of phenanthroline was calculated using the same approach. The assumption is that all mass lost during this process was due to phenanthroline. The mass loss $M_w \approx 162.07$ g/mol, suggests the loss of 0.90 moles of phenanthroline per mole of [Fe(phen)₃](SCN)₂.

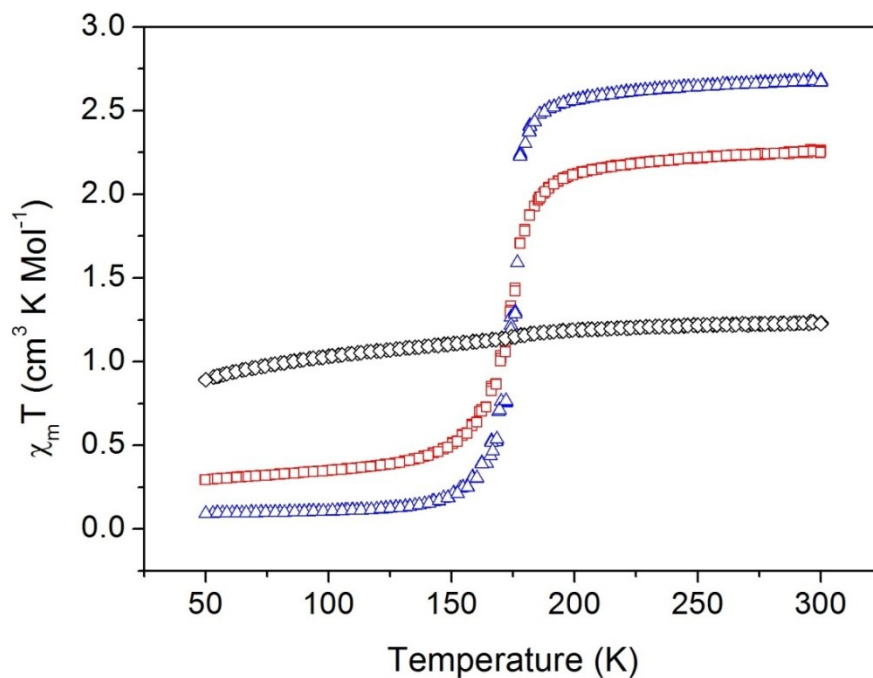


Figure S9: χ_{mT} vs T for $\mathbf{2}_{pre}$ (*), $\mathbf{2}_{mech}$ after thermolysis (\square) and $\mathbf{2}_{mech}$ after washing (Δ).

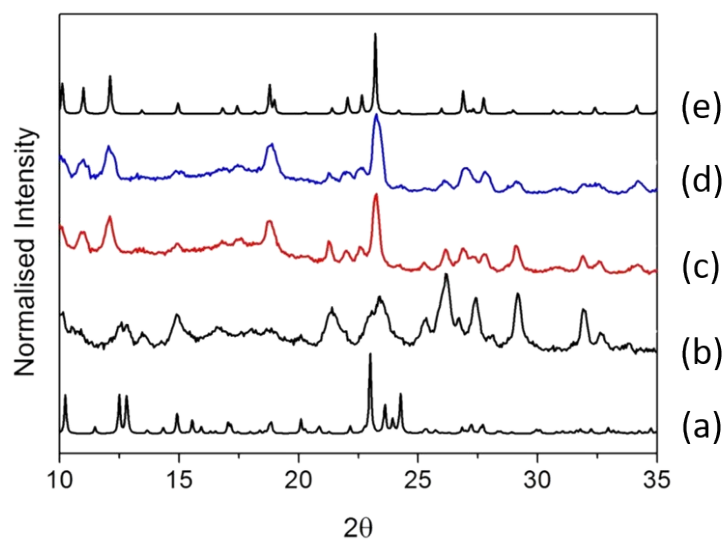


Figure S10: PXR D patterns: (a) $\mathbf{2}_{pre}$ (simulated from single crystal data), (b) $\mathbf{2}_{pre}$ (mechanochemically synthesised) (c) $\mathbf{2}_{mech}$ after thermolysis, (d) $\mathbf{2}_{mech}$ after thermolysis and subsequent washing, (e) $\mathbf{2}_{mech}$ (simulated from single crystal data)

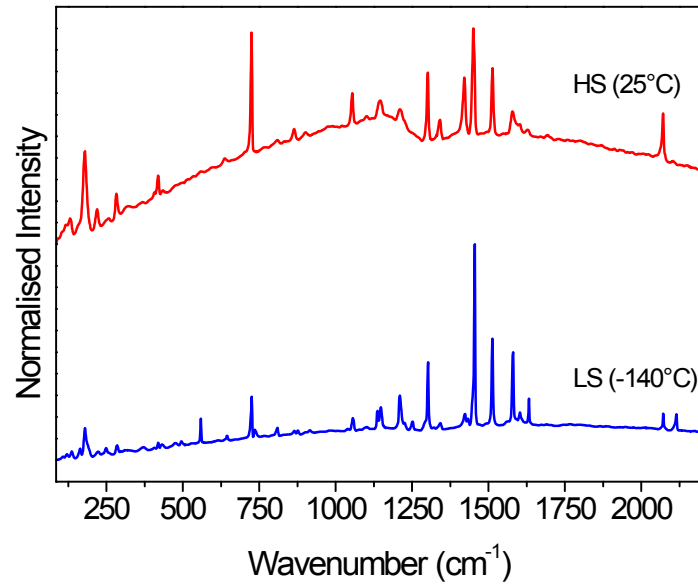


Figure S11: Variable temperature Raman spectra for 2_{mech} .

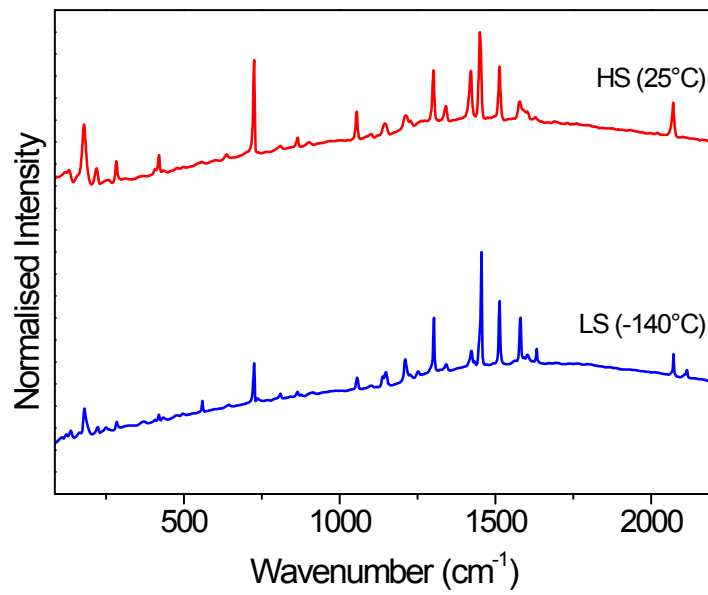


Figure S12: Variable temperature Raman spectra for 2_{mech} after washing.

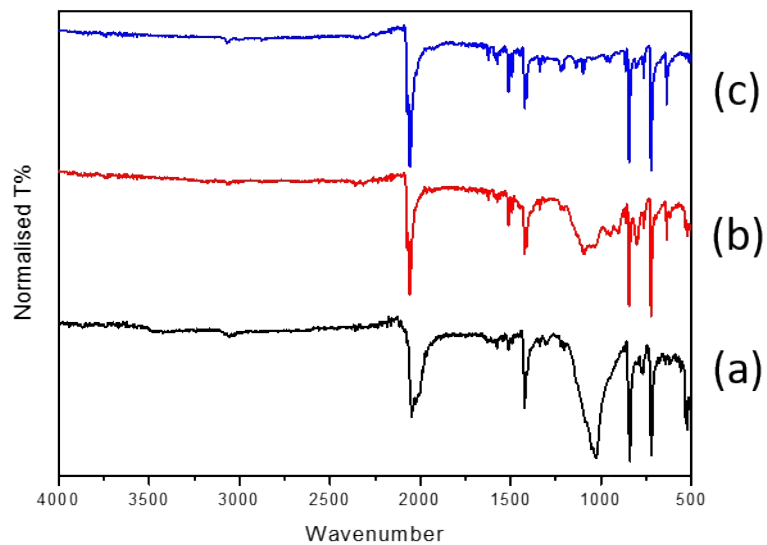


Figure S13: FTIR Spectra: (a) $\mathbf{2}_{pre}$ (b) $\mathbf{2}_{mech}$ and (c) $\mathbf{2}_{mech}$ after washing.

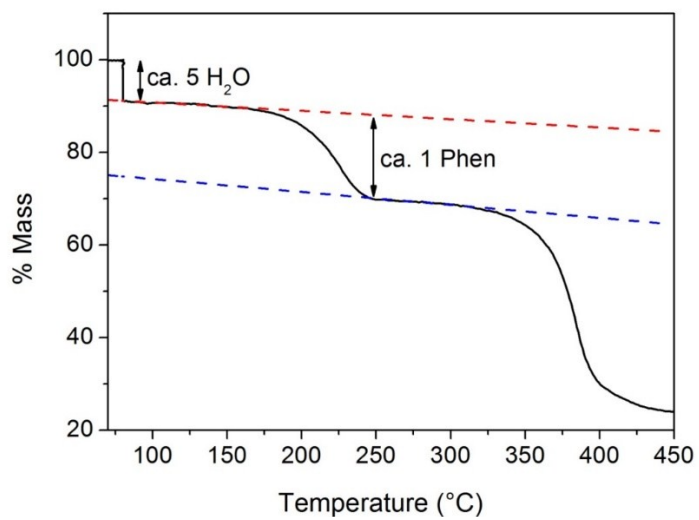


Figure S14: TGA for the conversion of $\mathbf{2}_{pre}$ to $\mathbf{2}_{mech}$ via thermolysis

Complex 3



The Raman spectrum in HS and LS states for $\mathbf{3}_{\text{mech}}$ is shown in figure S13, showing typical differences associated with the spin crossover phenomenon.

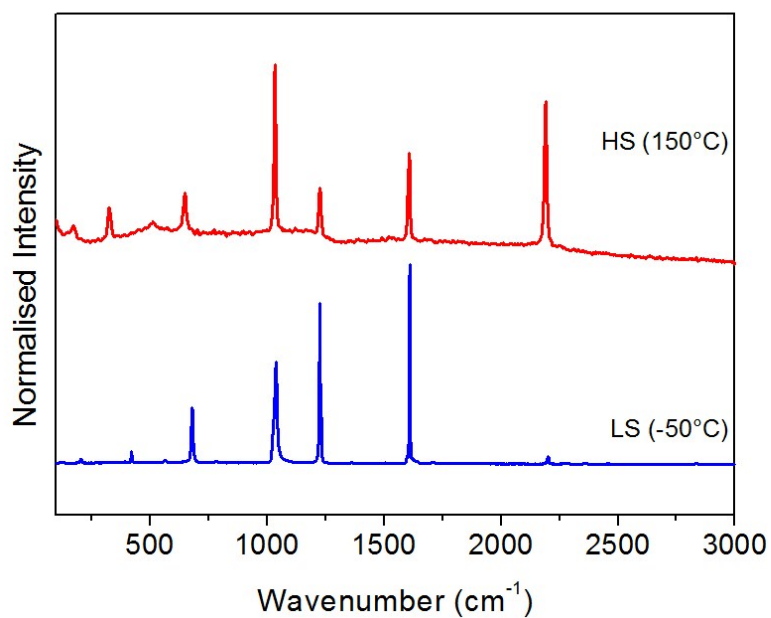


Figure S15: Variable Temperature Raman Spectra for $\mathbf{3}_{\text{mech}}$.

Complex 4

[Fe(atrz)₃](BF₄)₂

[Fe(atrz)₃](BF₄)₂ (complex **4**) is another member of the triazole-based SCO coordination polymers, and has the same 1D cationic chain structure as observed in compound **1**. The relatively gradual spin transition in this compound takes place around 200-250K, dependent on the exact synthetic procedure.³ It has been prepared more recently as nano-crystalline films by spray-drying.⁴ Here **4** was synthesised through mechanochemistry (**4**_{mech}) and from solution (**4**_{sol}) to allow comparison of properties as was done for **1** – **3** in the main text. The magnetometry data for **4**_{sol} is presented in Figure S16. The first cycle shows a small hysteresis ($T_{\frac{1}{2}\uparrow} = 234$, $T_{\frac{1}{2}\downarrow} = 227$ K). Subsequent cycles are shifted slightly in temperature and the hysteresis is significantly smaller ($T_{\frac{1}{2}\uparrow} = 249$, $T_{\frac{1}{2}\downarrow} = 245$ K, “Smoothness” = 12). By comparison **4**_{mech} shows ($T_{\frac{1}{2}\uparrow} = 230$ K, $T_{\frac{1}{2}\downarrow} = 225$ K, “Smoothness” = 19).

In general the conclusions are similar to complexes **1-3**; it is possible to make **4** via mechanochemistry to yield a material with very similar, if slightly less abrupt spin crossover behaviour. Like **1**, **4** is sensitive to the presence of residual water and requires high temperature drying to remove all traces of water. This is clear from magnetometry data for **4**_{mech} prior to drying (Figure S18), after drying (Figure S17) and after washing (Figure S19).

Differences in the structure are also apparent from the PXRD pattern presented in Figure S20. FTIR and Raman spectra of **4**_{mech} are shown in Figures S21 and S22 respectively. Differences in the structure are also apparent from the PXRD pattern presented in Figure S20. FTIR and Raman spectra of **4**_{mech} are shown in Figures S20 and S21 respectively.

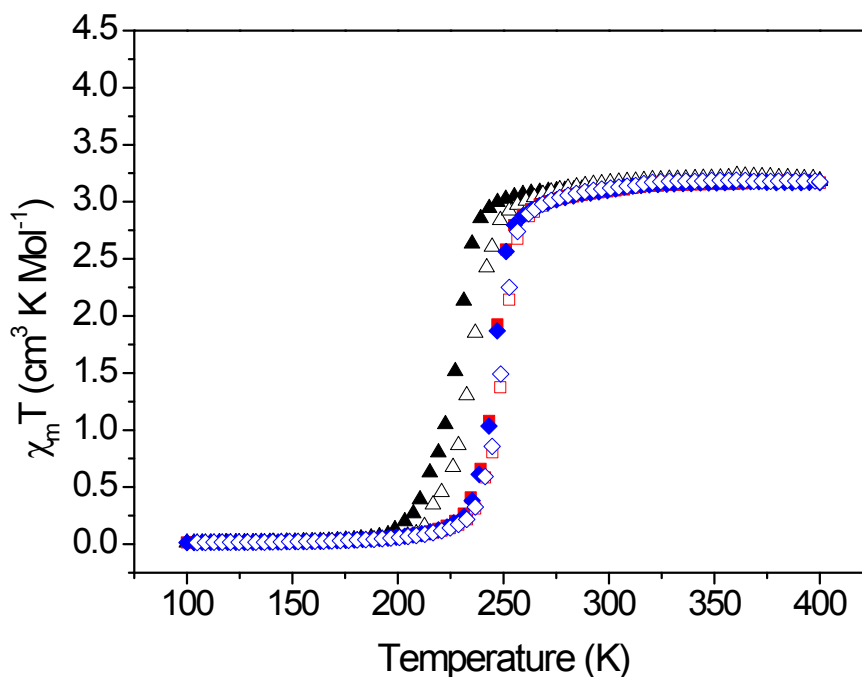


Figure S16: $\chi_M T$ vs T for **4**_{sol} as a function of temperature. 3 Cycles: \blacktriangle Cycle 1 Cool, \triangle Cycle 1 Heat, \blacksquare Cycle 2 Cool, \square Cycle 2 Heat, \blacklozenge Cycle 3 Cool and \ast Cycle 3 Heat.

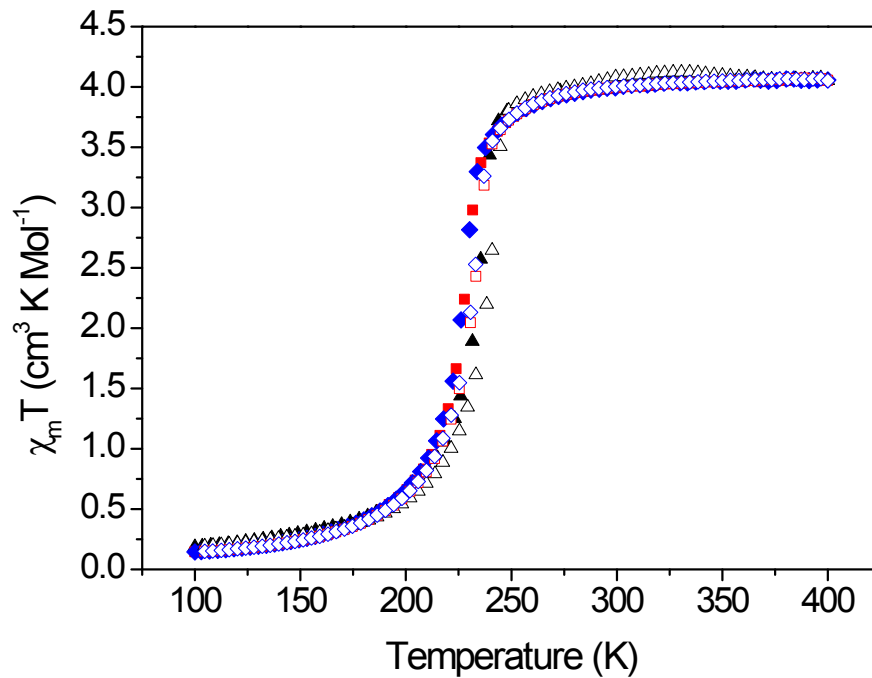


Figure S17: $\chi_m T$ vs T for 4_{mech} (after high temperature drying) as a function of temperature 3 Cycles: \blacktriangle Cycle 1 Cool, \triangle Cycle 1 Heat, \blacksquare Cycle 2 Cool, \square Cycle 2 Heat, \blacklozenge Cycle 3 Cool and \ast Cycle 3 Heat.

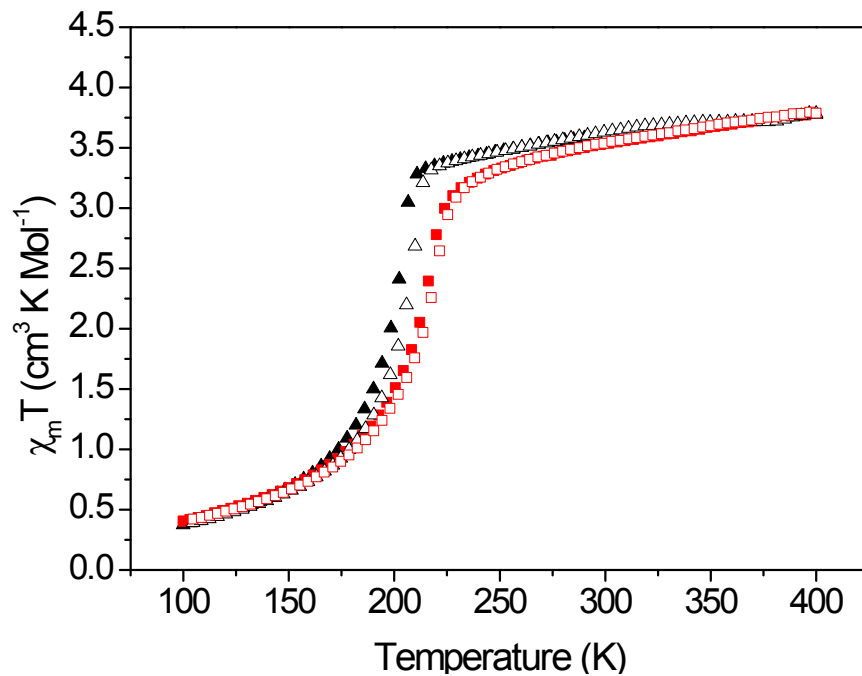


Figure S18: $\chi_m T$ vs T for 4_{mech} (prior to high temperature drying) as a function of temperature. 2 Cycles: \blacktriangle Cycle 1 Cool, \triangle Cycle 1 Heat, \blacksquare Cycle 2 Cool and \square Cycle 2 Heat.

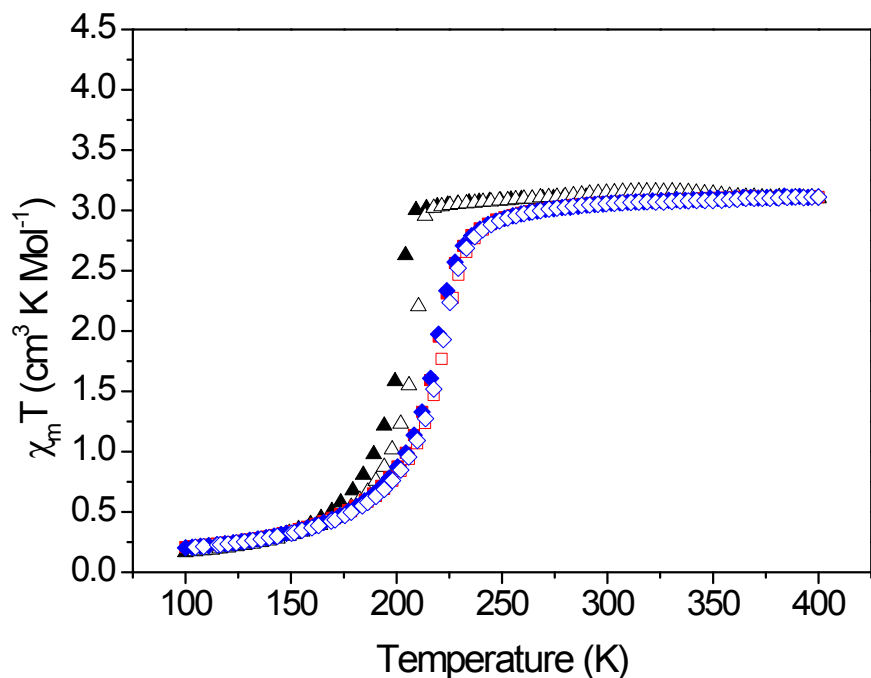


Figure S19: $\chi_{\text{m}}T$ vs T for 4_{mech} (after washing) as a function of temperature. 3 Cycles: \blacktriangle Cycle 1 Cool, \triangle Cycle 1 Heat, \blacksquare Cycle 2 Cool, \square Cycle 2 Heat, \blacklozenge Cycle 3 Cool and $*$ Cycle 3 Heat.

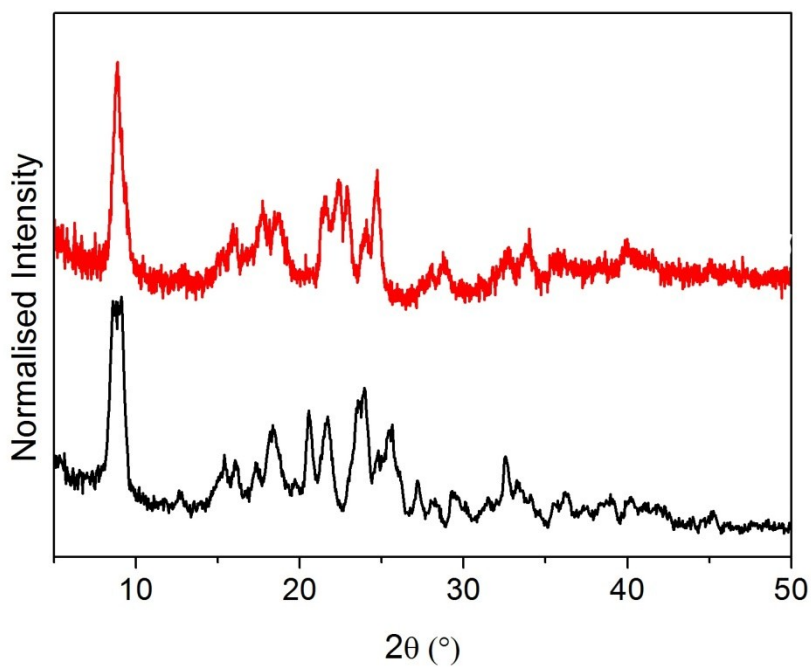


Figure S20: PXR D Patterns of 4_{mech} before (bottom) and after (top) high temperature drying.

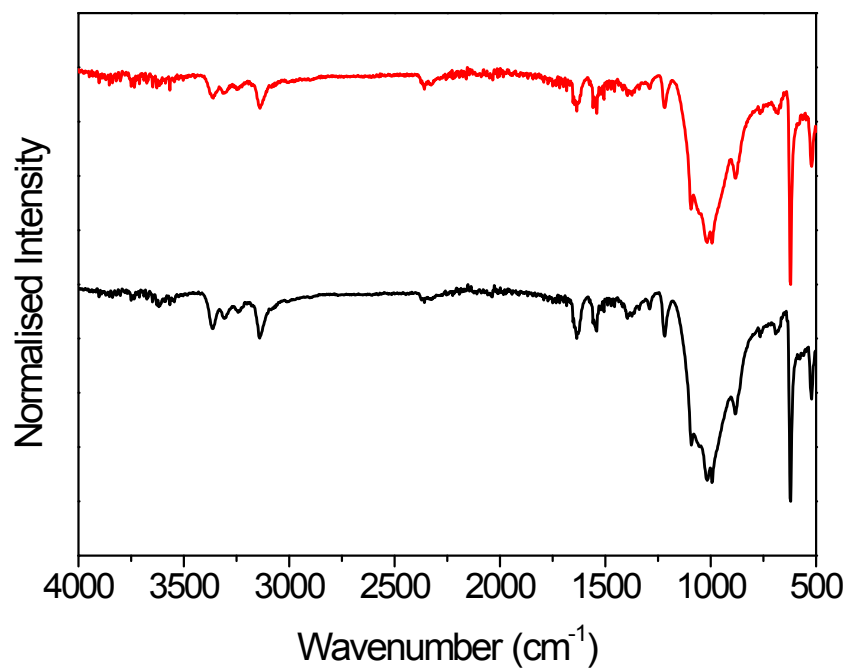


Figure S21: FTIR spectra of 4_{mech} before (bottom) and after (top) high temperature drying.

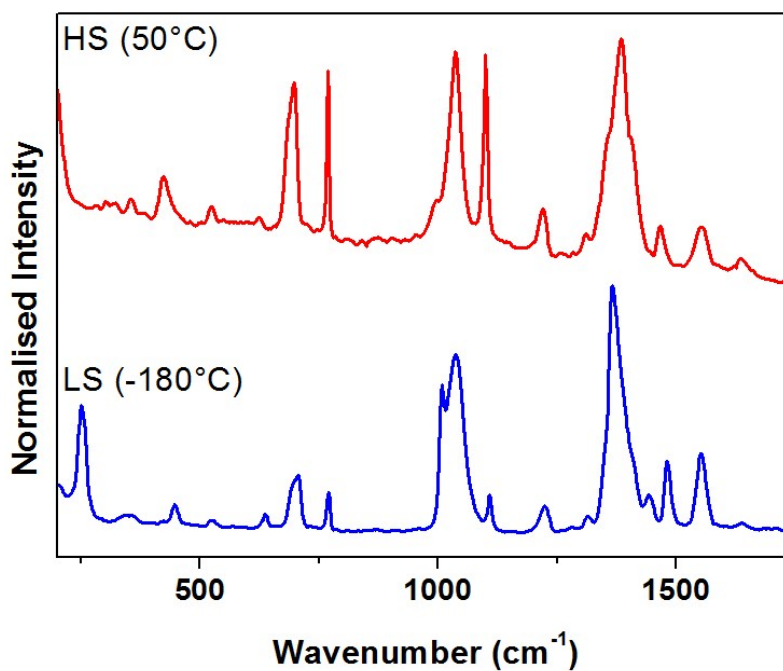


Figure S22: Variable Temperature Raman Spectra for 4_{mech} after high temperature drying.

¹ (a) E. C. Ellingsworth, B. Turner and G. Szulczewski, *RSC Adv.*, 2013, **3**, 3745–3754. (b) J. Laisney, A. Tissot, G. Molnár, L. Rechinat, E. Rivière, F. Brisset, A. Bousseksou, M.-L. Boillot, *Dalton Trans.*, 2015, **44**, 17302-17311

² O. Roubeau, *Chem. Eur. J.*, 2012, 15230

³ O. Kahn, J. Kröber and C. Jay, *Adv. Mater.*, 1992, **4**, 718–728.

⁴ N. Daro, L. Moulet, N. Penin, N. Paradis, J.-F. Létard, E. Lebraud, S. Buffière, G. Chastanet and P. Guionneau, *Materials*, 2017, **10**, 60